

Phase transition in a four-fermion interaction model under boundary conditions and electromagnetic effects

Emerson B. S. Corrêa*

*Instituto de Ciências Exatas, Universidade Federal do Sul e Sudeste do Pará,
ICE/UNIFESSPA, 68505-080, Marabá, Pará, Brazil*

 (Received 28 February 2023; accepted 11 July 2023; published 9 October 2023)

We have performed the study of the phase transition of an effective model of fermions describing interactions between quarks in D dimensions, taking into account effects induced by the finite size of the system, with periodic, quasiperiodic, and antiperiodic boundary conditions (PBC, QBC, ABC, respectively), chemical potential, and an external electromagnetic field. This has been done by generalized Matsubara formalism. Through the proper-time representation, the electric, magnetic, temperature, chemical potential, and finite size effects are written in terms of well-knowing functions and Jacobi theta functions. The gap equation of the system is numerically solved and we show the behavior of the system when the thermodynamic parameters of the model are changed. For fixed finite sizes, one of the findings is that the broken chiral symmetry is enhanced by the magnetic field increasing, but for the increasing electric field, we have the restoration of chiral symmetry. In fixed external fields, the influence of L on the phase transition is not unique: ABC conditions tend to restore chiral symmetry, while PBC conditions improve the broken phase and the QBC conditions have intermediate behavior, considering the same range of temperatures and L decreasing. We also observed little influence of finite chemical potential on the phase structure of the system and a minimal critical size of the system for ABC but not for QBC or PBC cases.

DOI: [10.1103/PhysRevD.108.076002](https://doi.org/10.1103/PhysRevD.108.076002)

I. INTRODUCTION

The quark gluon plasma (QGP) is a strongly interacting state of matter due to the compression and heating of hadronic matter. The QGP state arose microseconds after the big bang and can be observed directly after the heavy ion collisions [1–3]. Through quantum field theory (QFT), we can describe this state of matter at a finite temperature and volume. This description is given by the theory of strong interactions, quantum chromodynamics (QCD). However, the degrees of freedom of the gluons practically leave the theory with little possibility of presenting analytical results at average temperatures and chemical potentials.

Even though they are not renormalizable in four dimensions, effective models for QCD have been widely applied in extreme conditions of temperature and chemical potential, such as in the QGP. This applicability is thanks to the simpler mathematical structure of these models than QCD [4–7]. On effective models such as the Gross-Neveu [8] model and the Nambu-Jona-Lasinio (NJL) [9,10] model, there are no gluons and the quarks interact like points. These models present phase diagrams with the transition order parameter given by the chiral condensate. For this reason, we can analyze how the phase structure of the

model is modified when we change some thermodynamic parameters of the system on chiral condensate [11–16].

Important results arise when we consider effective models and thermodynamic variables such as temperature, chemical potential, finite size, and magnetic fields. For example, the NJL model presents the phenomenon of breaking/restoring chiral symmetry at finite temperature, in addition to satisfactorily describing mesons [17–19]. The behavior of a system with a finite size can differ significantly from that infinite one. Indeed, the GN model shows the occurrence of a minimum finite size, below which no first- or second-order phase transitions occur. This minimum finite size seems to be independent of the chemical potential [20–23]. Other important phenomena to consider are magnetic catalysis (i.e., an improvement in chiral symmetry breaking for an increasing magnetic field) [24–29] and inverse magnetic catalysis (an improvement in restoring chiral symmetry, again for an increasing magnetic field) [30–44].

In Ref. [45], the effects of finite size in a four-fermion interaction model, defined in dimensions D ($D \leq 3$) were described through the effective potential of the system, analyzing their phase structure in planes $\mu - T$ and $L - T$ without external fields. As finite size effects can exhibit significant fluctuations in the physical properties of a system compared to their bulk form values, in this manuscript we intend to investigate finite size effects in a four-fermion

*ecorrea@unifesspa.edu.br

model for some types of boundary conditions in spatial coordinate z , namely: periodic (PBC), quasiperiodic (QBC), and antiperiodic (ABC) boundary conditions, under a constant external electromagnetic field at finite temperature and chemical potential.

Specifically, this paper aims to study the chiral symmetry breaking restoration of a two-flavor NJL model under different boundary conditions in the direction parallel to the external electromagnetic field (z direction). For this, we will use the generalized Matsubara formalism [21]. The Matsubara formalism states that the fermionic field assumes odd frequencies in momentum-energy space. These odd frequencies come from Kubo-Martin-Schwinger (KMS) conditions applied to the fermionic field, which results in antiperiodic boundary conditions in the imaginary-time coordinate.

Let us focus on the topology of the system. Initially, the system defined in dimensions D is heated. In this case, we have the compactification of the imaginary-time coordinate τ , which will belong to a circle such that $\tau \in [0, \beta]$. We represent this compact by S^1 . Note that the topology of the system heated to temperature β^{-1} is described by $\Gamma_D^1 = S^1 \times \mathbf{R}^{D-1}$. If we do another compactification, then this time in the spatial coordinate j , we will have one more circle: $x_j \in [0, L_j]$. After two compactifications, the topology of the system is described by a *torus*: $\Gamma_D^2 = S^1 \times S^1 \times \mathbf{R}^{D-2}$ and we must apply the QFT defined in spaces with toroidal topologies [20,46–48]. In the present manuscript, we will use the proper-time representation [49] to solve the gap equation of the system subject to Feynman's rules modified by two compactifications S^1 . The reader will find similar approaches in Refs. [16,17,25].

The paper is structured as follows: In Sec. II, we present the Lagrangian density of the system. By the mean-field approximation and by Schwinger's proper-time method in a toroidal topology, we obtain the system gap equation taking into account the effects due to temperature, chemical potential, finite size, and an external electromagnetic field along the direction z . These effects are embedded into the system through the order parameter, ϕ .

In Sec. III, we define the phenomenological input of the model and fix some parameters to numerically solve the gap equation. We also show the phase structure of the system and compare the results obtained here with the data on lattice QCD. We make our final remarks in Sec. IV. We derive the expression for the chiral condensate under an external electromagnetic field in Appendix A. In Appendix B, we show that our results are consistent with findings at the bulk form and with both finite chemical potential and temperature in Refs. [50,51] for a pure electric field. To extract finite results from the model, we need to use a regulator. Therefore, we will use an ultraviolet cutoff on integral expressions involving the proper time.

Throughout the work, the system of natural units is assumed and we used a D -dimensional Euclidean space.

II. FORMALISM

A. The NJL model

The NJL-type Lagrangian density is given by [52]

$$\mathcal{L}_{\text{NJL}} = \bar{\psi}(i\cancel{\partial} - m_0)\psi + G_s[(\bar{\psi}\psi)^2 + (\bar{\psi}i\gamma_5\vec{\tau}\psi)^2], \quad (1)$$

with $\cancel{\partial} = \gamma_\mu \partial_\mu$, being γ_μ elements of the Clifford algebra in D dimensions in Euclidean space. The quarks fields $\psi = (u, d)^T$ carry $N_f = 2$ flavors with $N_c = 3$ colors. The matrices $\vec{\tau}$ are the Pauli matrices that act on isospin space, G_s represents the effective coupling constant in scalar and pseudoscalar channels, and here it is treated as the input parameter of the model.

We performed the computations within the mean-field approach. This methodology inserts in the interaction terms of Eq. (1), the approximation $(\bar{\psi}\Gamma\psi) \rightarrow \bar{\psi}\Gamma\psi + \langle \bar{\psi}\Gamma\psi \rangle$. In this case, we have $\Gamma = (I, i\gamma_5\vec{\tau})$. The channel considered here is scalar. This allows us to obtain an equation for the constituent mass of the quark M

$$M = m_0 - 2G_s\phi, \quad (2)$$

where the quark condensate ϕ is defined by

$$\phi \equiv \langle \bar{\psi}\psi \rangle = \text{Tr}[S_F(p)], \quad (3)$$

with the quark-dressed propagator in Euclidean space, written as

$$S_F(p) = \frac{(\cancel{p} - M)}{(p^2 + M^2)}.$$

The trace on Eq. (3) is over Dirac matrices, flavor, and color spaces. Recall the trace of an odd number of γ_μ is null. Accordingly, the chiral condensate becomes

$$\phi = -2^{D/2}MN_cN_f \int \frac{d^D p}{(2\pi)^D} \frac{1}{p^2 + M^2}. \quad (4)$$

By using the identity

$$\mathcal{O}^{-1} = \int_0^{+\infty} ds \exp(-s\mathcal{O}),$$

the chiral condensate can be rewritten as

$$\phi = -2^{D/2}MN_cN_f \int_0^\infty dS \int \frac{d^D p}{(2\pi)^D} \exp[-S(p^2 + M^2)], \quad (5)$$

where S is the proper-time parameter and $p^2 = p_\tau^2 + \vec{p}^2$ being \vec{p} a $(D-2)$ -dimensional vector.

B. Generalized Matsubara prescription

The KMS conditions establish that the fermionic field is antiperiodic in the imaginary-time coordinate

$$\psi(\tau, z, \vec{r}) = -\psi(\tau + \beta, z, \vec{r}).$$

Correspondingly, the Matsubara prescription introduces the temperature on the system by replacing on temporal momenta

$$p_\tau \rightarrow \omega_{n_\tau} \equiv \frac{\pi}{\beta}(2n_\tau + 1) - i\mu, \quad n_\tau = 0, \pm 1, \pm 2, \dots$$

$$\int \frac{dp_\tau}{2\pi} f(p_\tau, p_z, \vec{p}) \rightarrow \frac{1}{\beta} \sum_{n_\tau=-\infty}^{\infty} f(\omega_{n_\tau}, p_z, \vec{p}), \quad (6)$$

where β^{-1} is the temperature of the system and μ its chemical potential.

We emphasize that the KMS conditions for fermions impose antiperiodic boundary conditions on the ψ field only for the imaginary-time coordinate, τ . However, for the inclusion of finite size effects in the model, we do not need to use only antiperiodic boundary conditions in the spatial coordinates.

To include several kinds of spatial boundary conditions on z direction, we define the relation [45–47]

$$\psi(\tau, z, \vec{r}) = e^{-i\pi\alpha_z} \psi(\tau, z + L_z, \vec{r}),$$

where $\alpha_z = 0$ denotes periodic boundary conditions and $\alpha_z = 1$ fix antiperiodic boundary conditions, both in the

z direction. For intervals on which we have $0 < \alpha_z < 1$ the system will be subject to the so-called twisted boundary conditions.

Thus, the spatial momenta are recast by

$$p_z \rightarrow \omega_{n_z} \equiv \frac{\pi}{L_z}(2n_z) - i\mu_z; \quad \mu_z = i\frac{\pi}{L_z}\alpha_z$$

$$\int \frac{dp_z}{2\pi} f(p_\tau, p_z, \vec{p}) \rightarrow \frac{1}{L_z} \sum_{n_z=-\infty}^{\infty} f(p_\tau, \omega_{n_z}, \vec{p}), \quad (7)$$

where $n_z = 0, \pm 1, \pm 2, \dots$ and L_z is the length of the compactified spatial coordinate z . The generalized Matsubara prescription are then given by Eqs. (6) and (7) [17,20,21].

By performing the sum of Matsubara frequencies in Schwinger's formalism (for technical details, see Refs. [15,25]), we obtain the Jacobi theta functions [53,54]

$$\theta_2(u; q) = 2 \sum_{n=0}^{+\infty} q^{(n+1/2)^2} \cos[(2n+1)u],$$

$$\theta_3(u; q) = 1 + 2 \sum_{n=1}^{+\infty} q^{n^2} \cos(2nu). \quad (8)$$

Now, we will include the thermal and finite size effects in coordinates τ and z , respectively, i.e., $\tau \in [0, \beta]$ and $z \in [0, L_z]$. The shape of the system will be like a film of thickness L_z , maintained at a finite temperature.

By replacing the expressions Eqs. (6) and (7) in Eq. (5), chiral quark condensate gets reduced to

$$\phi(\beta, \mu, L_z, \mu_z, D) = -\frac{2^{D/2} M N_c}{(4\pi)^{(D-2)/2} \beta L_z} N_f \int_0^\infty \frac{dS}{S^{(D-2)/2}} \exp[-S(M^2 - \mu^2 - \mu_z^2)]$$

$$\times \theta_2\left[\frac{2\pi\mu S}{\beta}; \exp\left(-\frac{4\pi^2 S}{\beta^2}\right)\right] \theta_3\left[\frac{2\pi\mu_z S}{L_z}; \exp\left(-\frac{4\pi^2 S}{L_z^2}\right)\right]. \quad (9)$$

Note that we have done $(D-2)$ Gaussian integrals over the spatial momenta \vec{p} in Eq. (5).

In bulk form, the quark condensate reads

$$\phi(\beta, \mu, L_z \rightarrow \infty, D) = -\frac{2^{D/2} M N_c}{(4\pi)^{(D-1)/2} \beta} N_f \int_0^\infty \frac{dS}{S^{(D-1)/2}} \exp[-S(M^2 - \mu^2)] \theta_2\left[\frac{2\pi\mu S}{\beta}; \exp\left(-\frac{4\pi^2 S}{\beta^2}\right)\right]. \quad (10)$$

On the other hand, by computing just finite size effects (in the PBC, QBC, and ABC cases), we have

$$\phi(\beta \rightarrow \infty, L_z, \mu_z, D) = -\frac{2^{D/2} M N_c}{(4\pi)^{(D-1)/2} L_z} N_f \int_0^\infty \frac{dS}{S^{(D-1)/2}} \exp[-S(M^2 - \mu_z^2)] \theta_3\left[\frac{2\pi\mu_z S}{L_z}; \exp\left(-\frac{4\pi^2 S}{L_z^2}\right)\right]. \quad (11)$$

The system with no compactifications, i.e., no temperature and with infinite volume, has the following chiral condensate

$$\phi(\beta \rightarrow \infty, L_z \rightarrow \infty, D) = -\frac{2^{D/2} M N_c}{(4\pi)^{(D)/2}} N_f \int_0^\infty \frac{dS}{S^{D/2}} \exp[-S(M^2)]. \quad (12)$$

In the next subsection, we will include the magnetic and electric effects on the model.

C. Inclusion of magnetic and electric effects

At this moment let us include a constant electromagnetic field on the system. The electric and magnetic backgrounds will be implemented by minimal coupling prescription in Eq. (1), namely: $\partial_\mu \rightarrow \partial_\mu - i\hat{Q}_f A_\mu^{\text{ext}}$, where A_μ is the D

potential and \hat{Q}_f is the quark electric charge of flavor f , being $Q_u = -2Q_d = (2/3)e$. We use the gauge $A_\mu^{\text{ext}} = (izE_0, 0, xB_0, 0, 0, \dots, 0)$, which generates the homogeneous and constants fields, (E_0, B_0) along the direction z [52,55,56].

In Appendix A, we derived the expression of chiral condensate under the E_0 and B_0 external fields.

Then the chiral condensate under the electromagnetic background is given by

$$\begin{aligned} \phi(\omega_E, \omega_B) = & -\frac{2^{D/2}MN_c}{(4\pi)^{(D-4)/2}} \sum_{f=u}^d \int_0^\infty \frac{dS}{S^{(D-4)/2}} \exp[-S(M^2)] \\ & \times \int \frac{dp_\tau}{2\pi} \frac{dp_z}{2\pi} \frac{dp_x}{2\pi} \frac{dp_y}{2\pi} \exp \left\{ -S \left[(p_\tau^2 + p_z^2) \frac{\tan(\omega_{fE}S)}{\omega_{fE}S} + (p_x^2 + p_y^2) \frac{\tanh(\omega_{fB}S)}{\omega_{fB}S} \right] \right\}, \end{aligned} \quad (13)$$

where $\omega_{fE} \equiv |Q_f|E_0$ and $\omega_{fB} \equiv |Q_f|B_0$.

Applying the generalized Matsubara prescription over chiral condensate under a pure magnetic background [see Eq. (A7) in Appendix A], we obtain

$$\begin{aligned} \phi(\beta, \mu, L_z, \mu_z, D, \omega_B) = & -\frac{2^{D/2}MN_c}{4\pi(4\pi)^{(D-4)/2}\beta L_z} \sum_{f=u}^d \int_0^\infty \frac{dS}{S^{(D-4)/2}} \exp[-S(M^2 - \mu^2 - \mu_z^2)] \\ & \times \theta_2 \left[\frac{2\pi\mu S}{\beta}; \exp\left(-\frac{4\pi^2 S}{\beta^2}\right) \right] \theta_3 \left[\frac{2\pi\mu_z S}{L_z}; \exp\left(-\frac{4\pi^2 S}{L_z^2}\right) \right] [\omega_{fB} \coth(\omega_{fB}S)]. \end{aligned} \quad (14)$$

For a pure electric field [see Eq. (A8) in Appendix A], we have

$$\begin{aligned} \phi(\beta, \mu, L_z, \mu_z, D, \omega_E) = & -\frac{2^{D/2}MN_c}{4\pi(4\pi)^{(D-4)/2}\beta L_z} \sum_{f=u}^d \int_0^\infty \frac{dS}{S^{(D-2)/2}} \exp \left\{ -\left[SM^2 - (\mu^2 + \mu_z^2) \frac{\tan(\omega_{fE}S)}{\omega_{fE}} \right] \right\} \\ & \times \theta_2 \left[\frac{2\pi\mu \tan(\omega_{fE}S)}{\beta\omega_{fE}}; \exp\left(-\frac{4\pi^2 \tan(\omega_{fE}S)}{\beta^2\omega_{fE}}\right) \right] \\ & \times \theta_3 \left[\frac{2\pi\mu_z \tan(\omega_{fE}S)}{L_z\omega_{fE}}; \exp\left(-\frac{4\pi^2 \tan(\omega_{fE}S)}{L_z^2\omega_{fE}}\right) \right]. \end{aligned} \quad (15)$$

In bulk form, under thermal and magnetic effects, we get

$$\begin{aligned} \phi(\beta, \mu, L_z \rightarrow \infty, D, \omega_B) = & -\frac{2^{D/2}MN_c}{4\pi(4\pi)^{(D-3)/2}\beta} \sum_{f=u}^d \int_0^\infty \frac{dS}{S^{(D-3)/2}} \exp[-S(M^2 - \mu^2)] \\ & \times \theta_2 \left[\frac{2\pi\mu S}{\beta}; \exp\left(-\frac{4\pi^2 S}{\beta^2}\right) \right] [\omega_{fB} \coth(\omega_{fB}S)], \end{aligned} \quad (16)$$

and for the electric background

$$\begin{aligned} \phi(\beta, \mu, L_z \rightarrow \infty, D, \omega_E) = & -\frac{2^{D/2}MN_c}{4\pi(4\pi)^{(D-3)/2}\beta} \sum_{f=u}^d \int_0^\infty \frac{dS}{S^{(D-2)/2}} \sqrt{\omega_{fE} \cot(\omega_{fE}S)} \exp \left\{ -\left[SM^2 - (\mu^2) \frac{\tan(\omega_{fE}S)}{\omega_{fE}} \right] \right\} \\ & \times \theta_2 \left[\frac{2\pi\mu \tan(\omega_{fE}S)}{\beta\omega_{fE}}; \exp\left(-\frac{4\pi^2 \tan(\omega_{fE}S)}{\beta^2\omega_{fE}}\right) \right]. \end{aligned} \quad (17)$$

In the limit of zero temperature but with finite size effects and under a magnetic background, we have

$$\begin{aligned} \phi(\beta \rightarrow \infty, L_z, \mu_z, D, \omega_B) &= -\frac{2^{D/2}MN_c}{4\pi(4\pi)^{(D-3)/2}L_z} \sum_{f=u}^d \int_0^\infty \frac{dS}{S^{(D-3)/2}} \exp[-S(M^2 - \mu_z^2)] \\ &\times \theta_3\left[\frac{2\pi\mu_z S}{L_z}; \exp\left(-\frac{4\pi^2 S}{L_z^2}\right)\right] [\omega_{fB} \coth(\omega_{fB} S)], \end{aligned} \quad (18)$$

for a pure electric field, at zero temperature, we obtain

$$\begin{aligned} \phi(\beta \rightarrow \infty, L_z, \mu_z, D, \omega_E) &= -\frac{2^{D/2}MN_c}{4\pi(4\pi)^{(D-3)/2}L_z} \sum_{f=u}^d \int_0^\infty \frac{dS}{S^{(D-2)/2}} \sqrt{\omega_{fE} \cot(\omega_{fE} S)} \\ &\times \exp\left\{-\left[SM^2 - (\mu_z^2) \frac{\tan(\omega_{fE} S)}{\omega_{fE}}\right]\right\} \\ &\times \theta_3\left[\frac{2\pi\mu_z \tan(\omega_{fE} S)}{L_z \omega_{fE}}; \exp\left(-\frac{4\pi^2 \tan(\omega_{fE} S)}{L_z^2 \omega_{fE}}\right)\right]. \end{aligned} \quad (19)$$

Finally, at limits zero temperature and bulk form, we have, for the pure magnetic field case

$$\phi(\beta \rightarrow \infty, L_z \rightarrow \infty, D, \omega_B) = -\frac{2^{D/2}MN_c}{4\pi(4\pi)^{(D-2)/2}} \sum_{f=u}^d \int_0^\infty \frac{dS}{S^{(D-2)/2}} \exp[-S(M^2)] [\omega_{fB} \coth(\omega_{fB} S)], \quad (20)$$

and for the pure electric case, we have the following expression:

$$\phi(\beta \rightarrow \infty, L_z \rightarrow \infty, D, \omega_E) = -\frac{2^{D/2}MN_c}{4\pi(4\pi)^{(D-2)/2}} \sum_{f=u}^d \int_0^\infty \frac{dS}{S^{(D-2)/2}} \exp[-S(M^2)] [\omega_{fE} \cot(\omega_{fE} S)]. \quad (21)$$

As with the last remark, we note that, to regularize the integrals at proper time, we are adopting the ultraviolet cutoff Λ , which is defined as

$$\int_0^\infty f(S) dS \rightarrow \int_{1/\Lambda^2}^\infty f(S) dS. \quad (22)$$

In the next section, we perform the analysis of the phase structure of the system.

III. PHASE STRUCTURE

From now on, we will analyze the phase transition of the quarks system in interaction. Also, the chiral transition temperature as a function of finite size, electric, and magnetic backgrounds is investigated. Let us assume that $L_z = L$ and the parameters were fixed by fitting mass and pion decay constant in vacuum as $m_\pi = 0.138$ GeV and $f_\pi = 0.092$ GeV:

$$\begin{aligned} m_0 &= 0.005 \text{ GeV}; & \Lambda &= 0.776 \text{ GeV}; \\ G_s &= 4.730 \text{ GeV}^{-2}; & M_0 &= 0.350 \text{ GeV}. \end{aligned} \quad (23)$$

For the purposes of electromagnetic background, we use $M = (M_u + M_d)/2$. Furthermore, since estimated magnetic fields created on LHC and RHIC are in the range $m_\pi^2 < eB < 15m_\pi^2$, where m_π is the pion mass, here we fix three values of the external electromagnetic field for the plots. Let us fixed the size of the system in the z direction and investigate its behavior under T , and the cyclotron frequencies $\omega_E = eE_0$ and $\omega_B = eB_0$.

First of all, we will study the system at bulk form ($L \rightarrow \infty$). We can see the weak influence of chemical potential on the system in Fig. 1 for both finite magnetic and electric fields. We observe that the chemical potential (for a fixed external field) generates a smaller phase transition temperature (peak of thermal mass gradient) as μ increases. Also in the beginning and end of the range for T , the finite chemical potential does not make a difference with the approximation $\mu = 0.000$ GeV, for both magnetic and electric cases.

On the other hand, for fixed chemical potential ($\mu = 0.000$ GeV), we observe the increase of constituent quark mass and also the transition temperature, when the

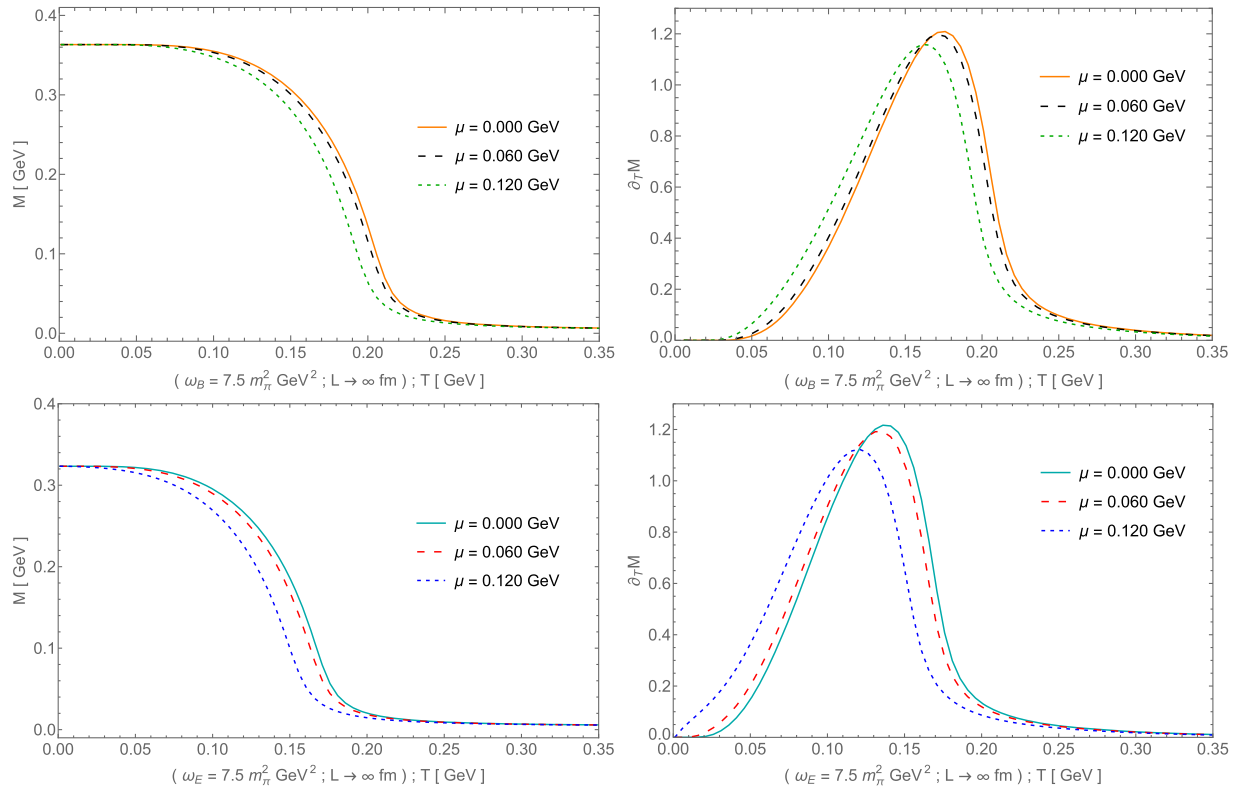


FIG. 1. Constituent quark mass as a function of temperature for three values of chemical potential in magnetic and electric fields fixed, with their respective thermal mass gradient.

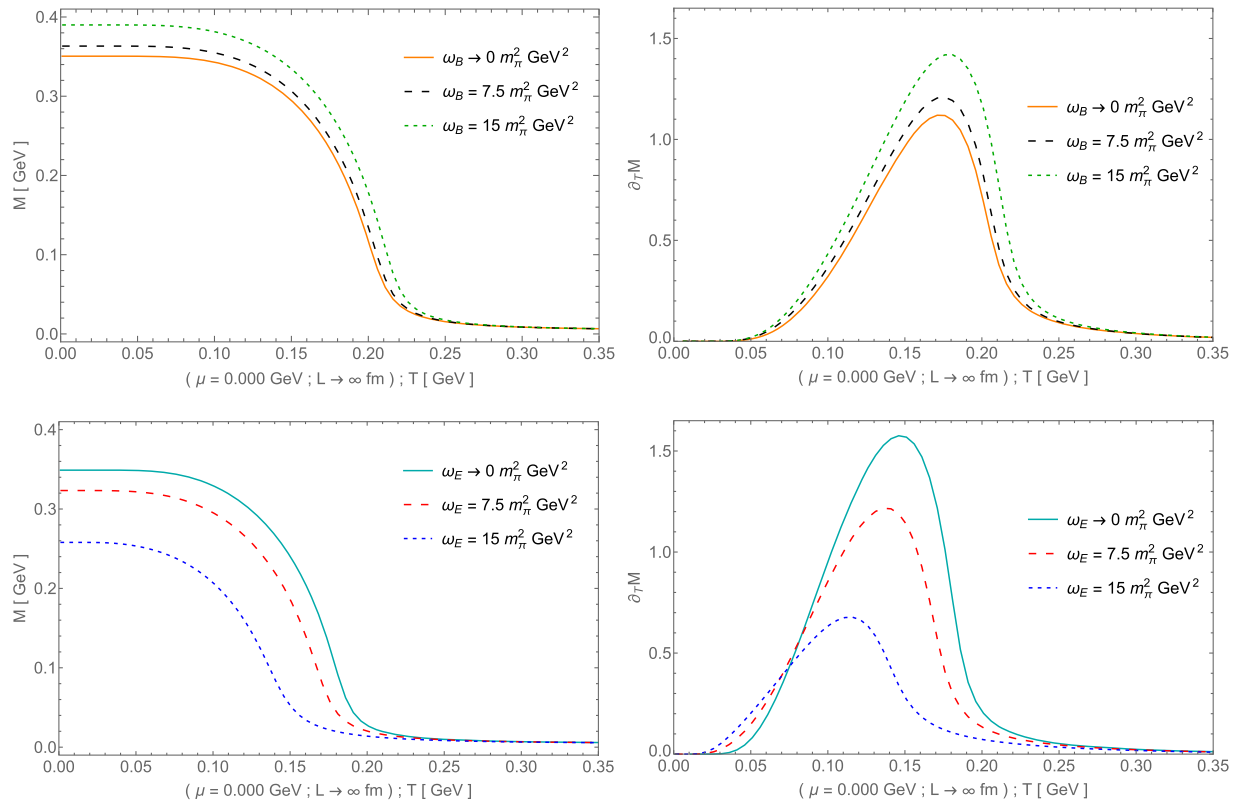


FIG. 2. Constituent quark mass as a function of temperature for magnetic and electric field strength with their respective thermal mass gradient.

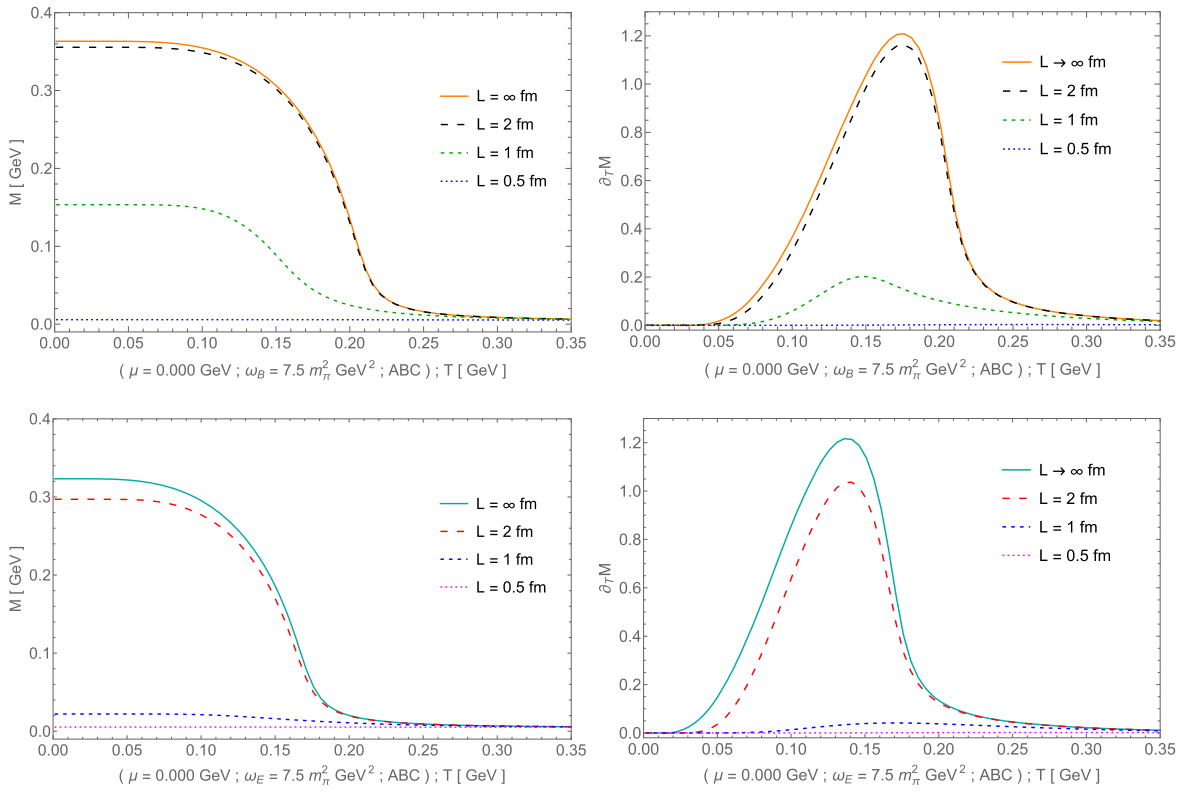


FIG. 3. Constituent quark mass as a function of temperature for several values of finite size and antiperiodic boundary conditions under magnetic and electric field strength with their respective mass gradient.

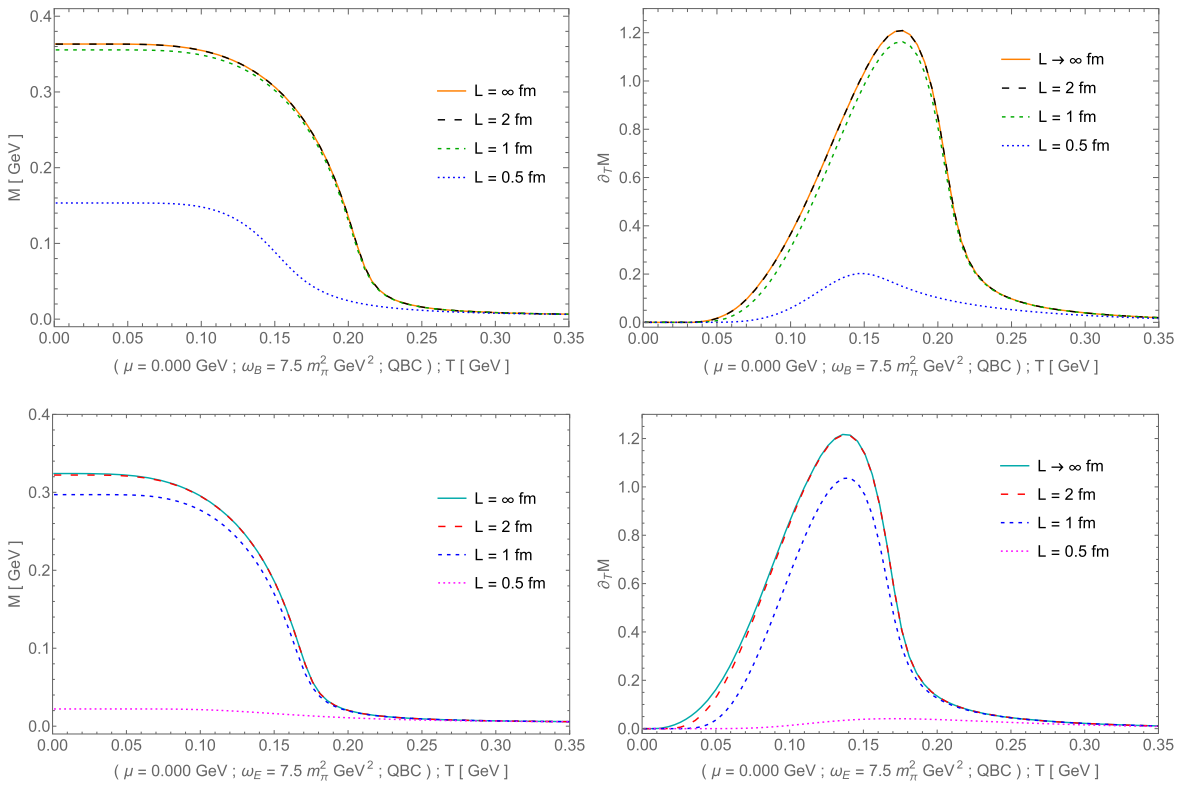


FIG. 4. Constituent quark mass as a function of temperature for several values of finite size and quasiperiodic boundary conditions under magnetic and electric field strength with their respective mass gradient.

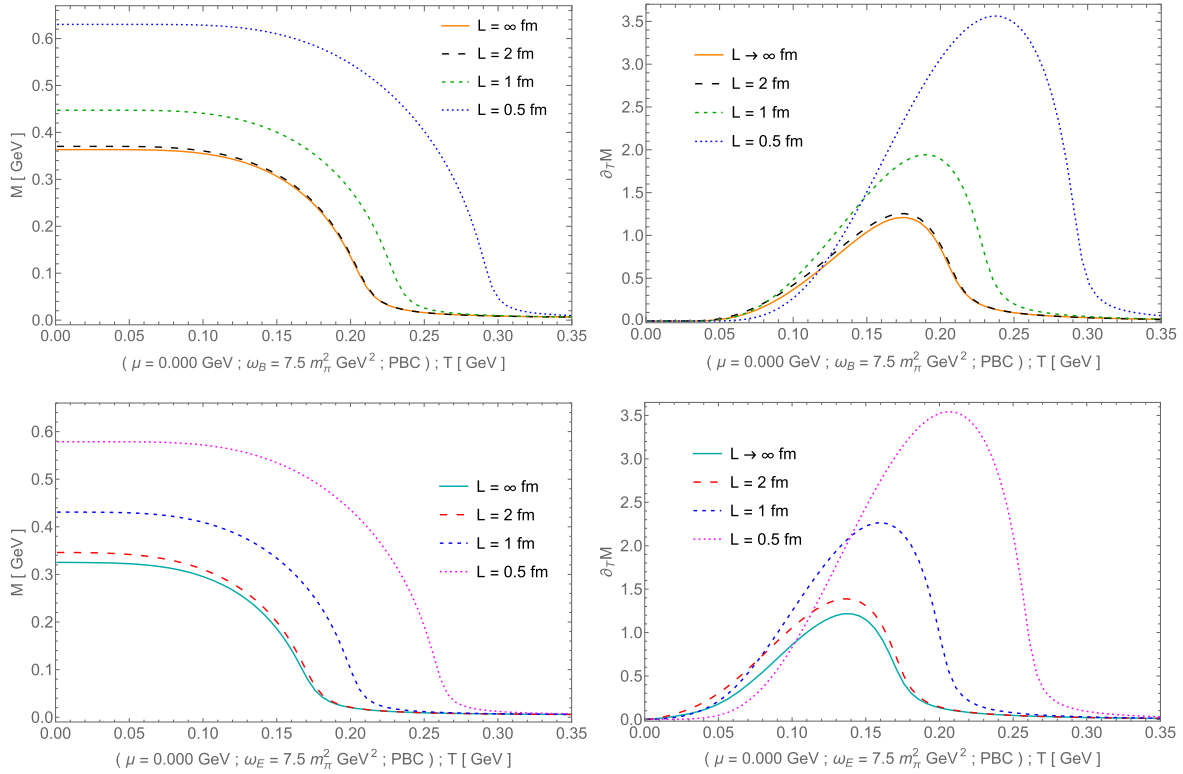


FIG. 5. Constituent quark mass as functions of temperature for several values of finite size and periodic boundary conditions under magnetic and electric field strength with their respective mass gradient.

magnetic field gets increases, i.e., we have the magnetic catalysis phenomena, as can be seen at the top plot of Fig. 2. Still, Fig. 2 (bottom plot), shows the behavior of the system under external electric fields. In this case, the transition temperature decreases for increases of ω_E . It is a kind of inverse electric catalysis.

The finite size effects are taken into account in Fig. 3. In that figure, we used antiperiodic boundary conditions and notice that ABC tend to restore the chiral symmetry when finite size gets decreased. Furthermore, the transition temperature assumes smaller values as finite size decrease. But, there is a L_c below that no chiral transition taking place. With the input given by Eq. (23), we find $L_c = 0.5$ fm.

In Fig. 4 we have the same as Fig. 3 but for quasiperiodic boundary conditions. The QBC case reveals that the bulk form has a good description by the finite size $L = 2$ fm. We notice that the quasiperiodic boundary condition effect on the system is lower transition temperatures as L decreases. But, the critical finite size is no anymore $L_c = 0.5$ fm. Actually, for $L = 0.5$ fm and QBC, we have chiral transition around $T = 0.150$ GeV for both $\omega_B = \omega_E = 7.5m_\pi^2$.

The periodic boundary conditions effects are considered on the system at Fig. 5. We notice the opposite behavior than in the ABC and QBC cases, namely as the finite size decrease, the constituent quark mass get increasing.

Thus, the PBC case reinforces the broken phase. Besides that, the transition temperatures assume higher values as the finite size of the system diminishes.

In Fig. 6, we fix $L = 1$ fm and $L = 0.5$ fm for the three different kinds of boundary conditions under the external fields ω_B and ω_E . This figure shows again the opposite behavior of the system under magnetic and electric external fields, i.e., magnetic catalysis and inverse electric catalysis, respectively. Also, we see that the critical finite size $L_c = 0.5$ fm, which does not allow the chiral transition for the ABC case, does not present any restriction for QBC and PBC cases.

Now, let us study the behavior of the system for a continuum range of finite sizes. This can be seen in Figs. 7 and 8 for fixed temperatures and fields.

We see from Figs. 7 and 8, that there is a $(1/L)_{\max}$ (or equivalently L_{\min}) above which (below which) cases ABC, QBC, and PBC get divergent values for M and $\partial_T M$. In other words, there is no difference in the constituent quark mass and in their respective thermal gradients for the cases ABC, QBC, or PBC in the interval from $L \rightarrow \infty$ to L_{\min} . The differences between the three types of boundary conditions imposed on the system arise for finite sizes smaller than L_{\min} . We show in Tables I and II, some theoretical values for L_{\min} obtained from solutions of gap equation (2). In Table I we present values of L_{\min} when the system is under a pure magnetic

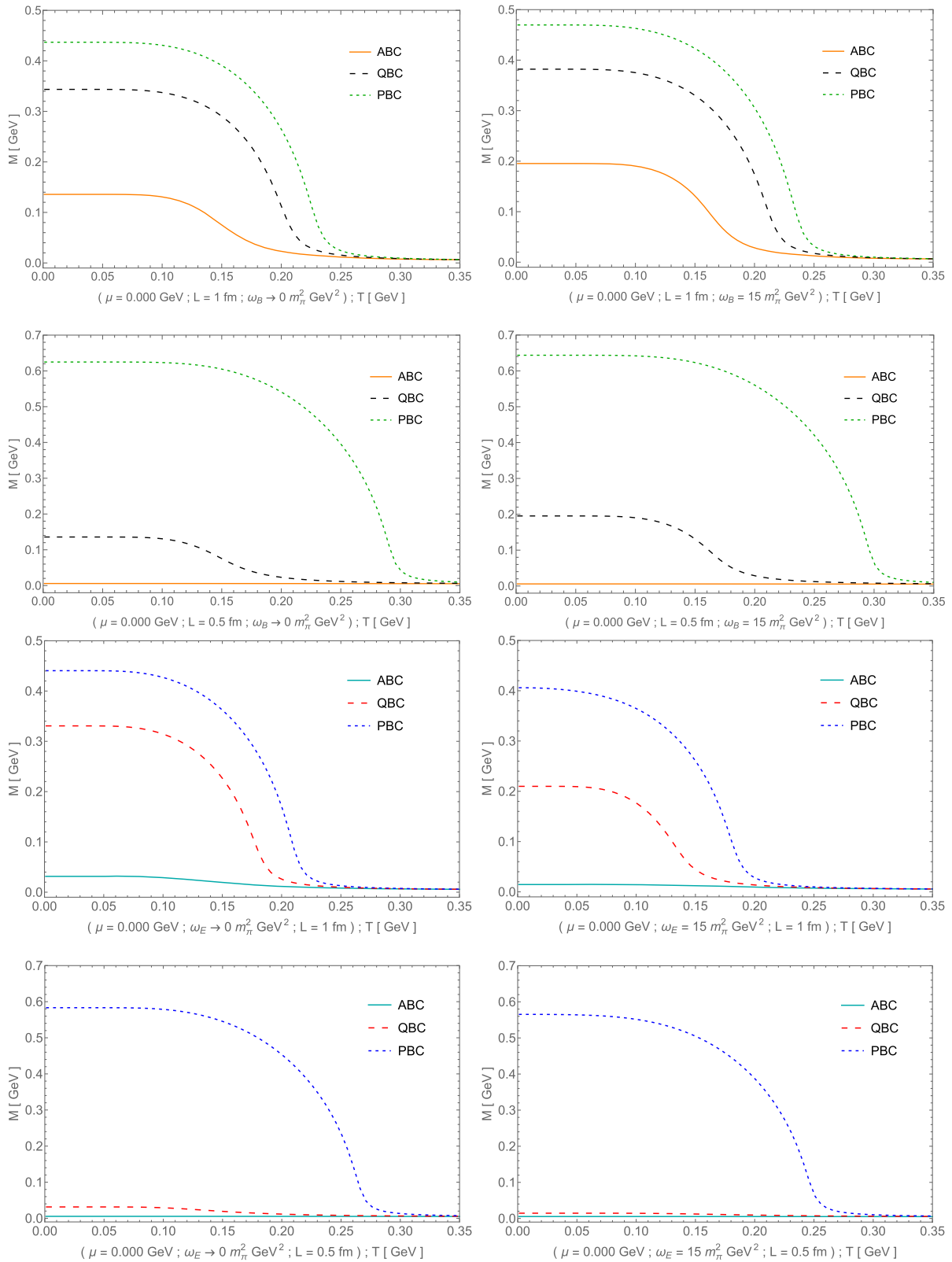


FIG. 6. Constituent quark mass as functions of temperature for three different boundary conditions under magnetic and electric fields for fixed finite sizes $L = 1$ fm and $L = 0.5$ fm.

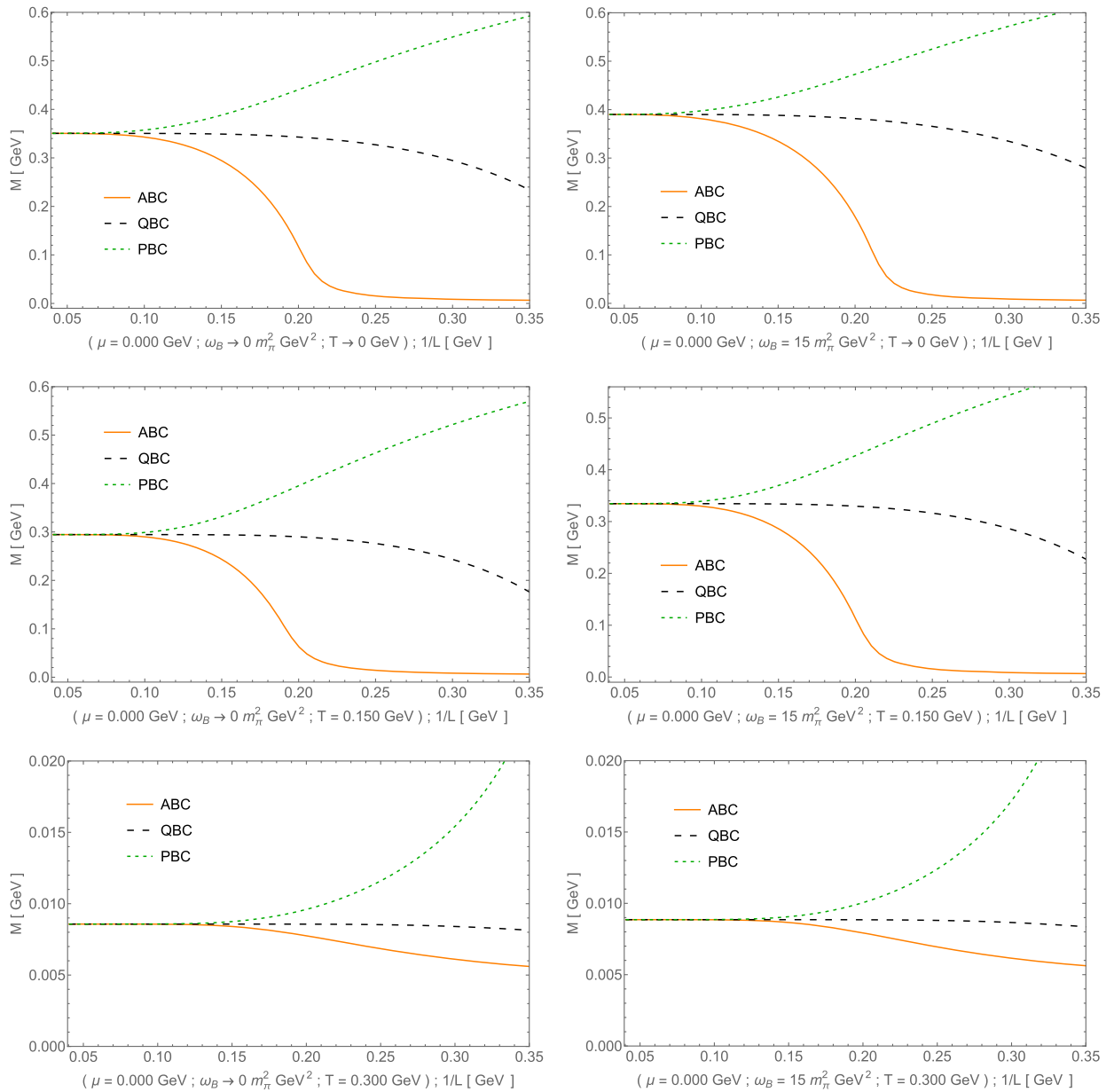


FIG. 7. Constituent quark mass as a function of the inverse of length for three different boundary conditions under magnetic fields for fixed temperatures $T \rightarrow 0$ GeV, $T = 0.150$ GeV, and $T = 0.300$ GeV.

field. Table II are show the minimum thickness for a pure electric field.

To finish our analysis, let us compare our results with lattice QCD (LQCD) at finite temperature and magnetic fields (continuum extrapolated results) [57]. In Figs. 9 and 10, we show the values of constituent quark mass normalized by M_0 in the bulk form with no chemical potential obtained here for several values of temperature and the corresponding ones in LQCD.

From the analysis of Figs. 9 and 10, we infer that the model considered in this work obtained a reasonable description for an effective model when compared with lattice QCD data for temperatures until 0.130 GeV. From this temperature value, we see discrepancies between LQCD and the four-fermion model considered here. The LQCD results close to the pseudocritical temperature (around 0.153 GeV in Fig. 10), show inverse magnetic catalysis.

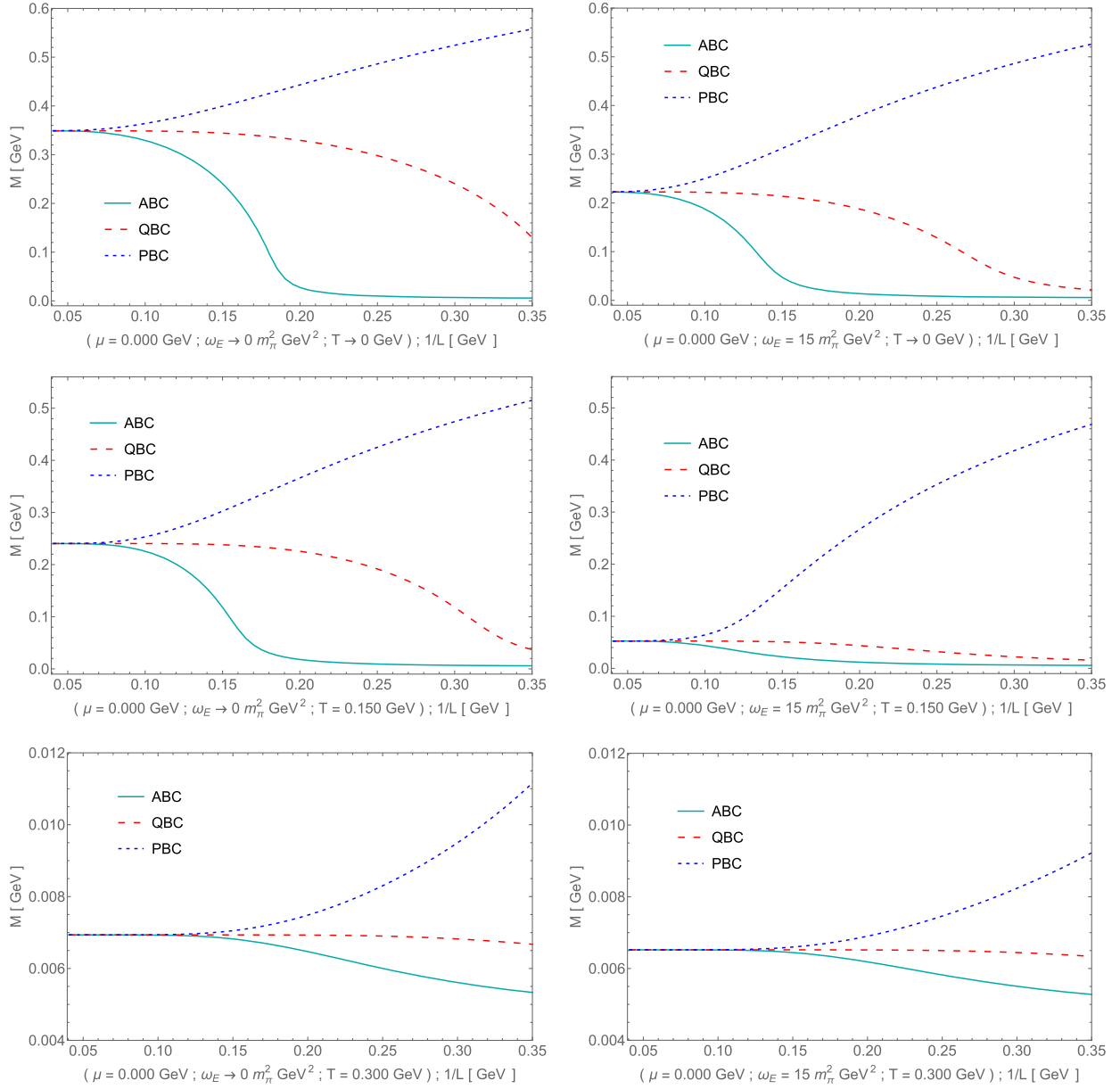


FIG. 8. Constituent quark mass as functions of the inverse of length for three different boundary conditions under electric fields for fixed temperatures $T \rightarrow 0$ GeV, $T = 0.150$ GeV, and $T = 0.300$ GeV.

IV. CONCLUSIONS

In this paper, we have applied QFT in a toroidal topology for studied finite size, chemical potential, and electromagnetic effects on the phase structure of the NJL model with

TABLE I. For $L > L_{\min}$ there are no differences between the ABC, QBC, and PBC cases under a magnetic field applied.

| No electric field | $T \rightarrow 0$ GeV | $T = 0.150$ GeV | $T = 0.300$ GeV |
|----------------------------------|-----------------------|----------------------|----------------------|
| $\omega_B \rightarrow 0 m_\pi^2$ | $L_{\min} = 2.98$ fm | $L_{\min} = 2.43$ fm | $L_{\min} = 1.71$ fm |
| $\omega_B = 15 m_\pi^2$ | $L_{\min} = 3.13$ fm | $L_{\min} = 2.66$ fm | $L_{\min} = 1.74$ fm |

two flavors and three colors. The little influence of chemical potential on the system is realized just for intermediate temperatures. At the beginning and at the end of the range for temperatures $[0, 0.350$ GeV] there is no

TABLE II. For $L > L_{\min}$ there are no differences between the ABC, QBC, and PBC cases under an electric field applied.

| No magnetic field | $T \rightarrow 0$ GeV | $T = 0.150$ GeV | $T = 0.300$ GeV |
|----------------------------------|-----------------------|----------------------|----------------------|
| $\omega_E \rightarrow 0 m_\pi^2$ | $L_{\min} = 3.79$ fm | $L_{\min} = 3.39$ fm | $L_{\min} = 1.95$ fm |
| $\omega_E = 15 m_\pi^2$ | $L_{\min} = 3.95$ fm | $L_{\min} = 3.45$ fm | $L_{\min} = 2.01$ fm |

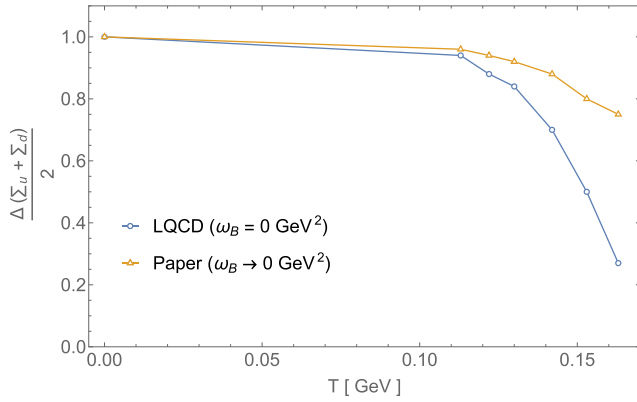


FIG. 9. Results obtained here and the data from lattice QCD taken from Ref. [57] at vanishing magnetic field.

difference in the values of constituent quark mass and their respective thermal gradient when we considered finite or zero chemical potential.

We have found the magnetic catalysis phenomenon for antiperiodic, quasiperiodic, and periodic boundary conditions at spatial coordinate z in a continuum range of L (see Fig. 7). Under a pure electric field, we have found the inverse electric catalysis, i.e., the decrease of effective quark mass for an electric field increasing, again for the three types of boundary conditions in a continuum range of finite size (see Fig. 8).

From a physical point of view, the chiral condensate is enhanced by the magnetic field, since the pair quark-antiquark has opposite spins, which tend to get alignment to the magnetic field. On the other hand, for an electric external field, the different electric charges of the pair tend to separate the chiral condensate in virtue of electric force [5].

Furthermore, for T or fixed external fields, decreasing L tends to restore chiral symmetry, for ABC. But, taking into account the PBC case, for smaller L , we have that the chiral symmetry breaking is reinforced. For the QBC case, we observe an intermediate behavior between the ABC and PBC cases such that $M_{ABC} < M_{QBC} < M_{PBC}$ for the same set of thermodynamic parameters $(\omega_B, \omega_E, T, \mu, L)$.

The findings in this manuscript and the lattice QCD data were compared in Figs. 9 and 10 for the cases of null and non-null magnetic fields, respectively. Our results showed

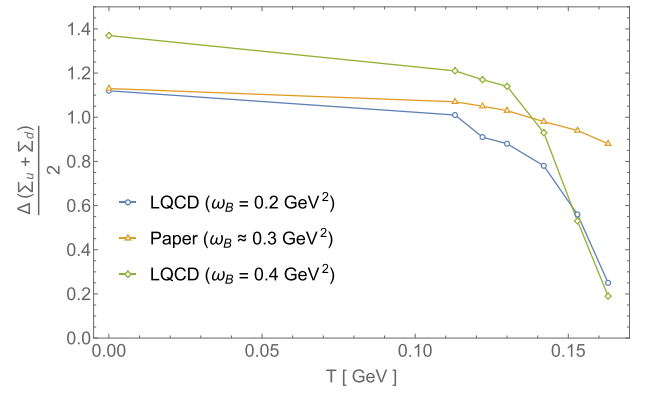


FIG. 10. Results obtained here for $\omega_B = 15m_\pi^2$ and the data from lattice QCD taken from Ref. [57] at the finite magnetic field.

reasonable agreement with LQCD for a temperature from zero to 0.130 GeV. Above this temperature, the effective model treated here and the LQCD data started to drift apart.

The thermodynamic description of a system taking into account its finite size, temperature, chemical potential, and an external electromagnetic field, reveals important effects such as restoration/breaking of chiral symmetry, magnetic catalysis, and inverse electric catalysis. We will continue studying these interesting effects on other models and backgrounds.

ACKNOWLEDGMENTS

E. B. S. C. would like to thank both Michelli Sarges for instigating him to write this paper and the anonymous referee for helpful comments.

APPENDIX A: CHIRAL CONDENSATE UNDER AN ELECTROMAGNETIC EXTERNAL FIELD

In this Appendix, we shall calculate the chiral condensate in the gauge $A_\mu^{\text{ext}} = (izE_0, 0, xB_0, 0, 0, \dots, 0)$. It is defined by

$$\phi = \text{Tr}[S_F(p, A^{\text{ext}})], \quad (\text{A1})$$

being the propagator on the momentum space given by [58,59]

$$S_F(p, A^{\text{ext}}) = \frac{i}{16\pi^2} \int \frac{d^{D-4}p}{(2\pi)^{D-4}} \omega_{fE} \omega_{fB} \sum_{\ell, \ell'=0}^{+\infty} \sum_{\sigma_E, \sigma_B=\pm 1} \frac{(\not{p} - M)}{i\omega_{fE}(2\ell + 1 + \sigma_E) + \omega_{fB}(2\ell' + 1 + \sigma_B) + \vec{p}^2 + M^2}, \quad (\text{A2})$$

where ℓ and ℓ' are the Landau levels, σ_E and σ_B are the spin variables, besides that $\omega_{fE} \equiv |Q_f|E_0$ and $\omega_{fB} \equiv |Q_f|B_0$.

Taking the trace and considering the representation of proper time, we get

$$\begin{aligned} \phi(\omega_E, \omega_B) = & -\frac{i2^{D/2}MN_c}{16\pi^2} \sum_{f=u}^d \int_0^\infty dS \int \frac{d^{D-4}p}{(2\pi)^{D-4}} \omega_{fE}\omega_{fB} \exp[-S(\vec{p}^2 + M^2)] \\ & \times \sum_{\ell, \ell'=0}^{+\infty} \sum_{\sigma_E, \sigma_B=\pm 1} \exp\{-S[i\omega_{fE}(2\ell+1+\sigma_E) + \omega_{fB}(2\ell'+1+\sigma_B)]\}. \end{aligned} \quad (\text{A3})$$

Performing the geometrical sums on the Landau levels and on the spin variables, we have

$$\begin{aligned} \phi(\omega_E, \omega_B) = & -\frac{i2^{D/2}MN_c}{16\pi^2} \sum_{f=u}^d \int_0^\infty dS \int \frac{d^{D-4}p}{(2\pi)^{D-4}} \omega_{fE}\omega_{fB} \exp[-S(\vec{p}^2 + M^2)] \\ & \times \left\{ \left[\frac{\exp(2i\omega_{fE}S)}{-1 + \exp(2i\omega_{fE}S)} \right] + \left[\frac{1}{-1 + \exp(2i\omega_{fE}S)} \right] \right\} \\ & \times \left\{ \left[\frac{\exp(2\omega_{fB}S)}{-1 + \exp(2\omega_{fB}S)} \right] + \left[\frac{1}{-1 + \exp(2\omega_{fB}S)} \right] \right\}. \end{aligned} \quad (\text{A4})$$

Finally, after some simple steps, we can write Eq. (A4) as

$$\phi(\omega_E, \omega_B) = -2^{D/2}MN_c \sum_{f=u}^d \int_0^\infty dS \int \frac{d^{D-4}p}{(2\pi)^{D-4}} \frac{\omega_{fE}}{4\pi} \frac{\omega_{fB}}{4\pi} \exp[-S(\vec{p}^2 + M^2)] \cot(\omega_{fE}S) \coth(\omega_{fB}S). \quad (\text{A5})$$

The vector \vec{p} is a $(D-4)$ -dimensional vector. This dimensional reduction takes place due to including the external fields parallel to the z direction. The electric field couples the τ and z coordinates (in the momenta space, p_τ and p_z) while the magnetic field couples the x and y coordinates (in the momenta space, p_x and p_y). Notwithstanding, we can recompose the D dimensions of the propagator using the well-known relations

$$\int_{-\infty}^{+\infty} \int_{-\infty}^{+\infty} \frac{dp_\tau}{2\pi} \frac{dp_z}{2\pi} \exp\left[-(p_\tau^2 + p_z^2) \frac{\tan(\omega_{fE}S)}{\omega_{fE}}\right] = \frac{\omega_{fE}}{4\pi} \cot(\omega_{fE}S),$$

and

$$\int_{-\infty}^{+\infty} \int_{-\infty}^{+\infty} \frac{dp_x}{2\pi} \frac{dp_y}{2\pi} \exp\left[-(p_x^2 + p_y^2) \frac{\tanh(\omega_{fB}S)}{\omega_{fB}}\right] = \frac{\omega_{fB}}{4\pi} \coth(\omega_{fB}S).$$

Therefore, the chiral condensate at zero temperature under magnetic and electric backgrounds reads

$$\begin{aligned} \phi(\omega_E, \omega_B) = & -2^{D/2}MN_c \sum_{f=u}^d \int_0^\infty dS \int \frac{d^{D-4}p}{(2\pi)^{D-4}} \exp[-S(\vec{p}^2 + M^2)] \\ & \times \int \frac{dp_\tau}{2\pi} \frac{dp_z}{2\pi} \frac{dp_x}{2\pi} \frac{dp_y}{2\pi} \exp\left\{-S\left[(p_\tau^2 + p_z^2) \frac{\tan(\omega_{fE}S)}{\omega_{fE}} + (p_x^2 + p_y^2) \frac{\tanh(\omega_{fB}S)}{\omega_{fB}}\right]\right\}, \end{aligned}$$

after $(D-4)$ Gaussian integrals, we have

$$\begin{aligned} \phi(\omega_E, \omega_B) = & -\frac{2^{D/2}MN_c}{(4\pi)^{(D-4)/2}} \sum_{f=u}^d \int_0^\infty \frac{dS}{S^{(D-4)/2}} \exp[-S(M^2)] \\ & \times \int \frac{dp_\tau}{2\pi} \frac{dp_z}{2\pi} \frac{dp_x}{2\pi} \frac{dp_y}{2\pi} \exp\left\{-S\left[(p_\tau^2 + p_z^2) \frac{\tan(\omega_{fE}S)}{\omega_{fE}} + (p_x^2 + p_y^2) \frac{\tanh(\omega_{fB}S)}{\omega_{fB}}\right]\right\}. \end{aligned} \quad (\text{A6})$$

Let us take the limit of Eq. (A6) for pure magnetic field ($\omega_E = eE_0 \rightarrow 0$). In this case, the factor $[\tan(\omega_{fE}S)/\omega_{fE}S] \rightarrow 1$ allows us to write

$$\begin{aligned} \phi(0, \omega_B) &= -\frac{2^{D/2}MN_c}{(4\pi)^{(D-4)/2}} \sum_{f=u}^d \int_0^\infty \frac{dS}{S^{(D-4)/2}} \exp[-S(M^2)] \\ &\quad \times \int \frac{dp_\tau}{2\pi} \frac{dp_z}{2\pi} \frac{dp_x}{2\pi} \frac{dp_y}{2\pi} \exp \left\{ -S \left[(p_\tau^2 + p_z^2) + (p_x^2 + p_y^2) \frac{\tanh(\omega_{fB}S)}{\omega_{fB}S} \right] \right\}. \end{aligned} \quad (\text{A7})$$

In the same way, the limit of Eq. (A6) for pure electric field ($\omega_B = eB_0 \rightarrow 0$) gives

$$\begin{aligned} \phi(\omega_E, 0) &= -\frac{2^{D/2}MN_c}{(4\pi)^{(D-4)/2}} \sum_{f=u}^d \int_0^\infty \frac{dS}{S^{(D-4)/2}} \exp[-S(M^2)] \\ &\quad \times \int \frac{dp_\tau}{2\pi} \frac{dp_z}{2\pi} \frac{dp_x}{2\pi} \frac{dp_y}{2\pi} \exp \left\{ -S \left[(p_\tau^2 + p_z^2) \frac{\tan(\omega_{fE}S)}{\omega_{fE}S} + (p_x^2 + p_y^2) \right] \right\}. \end{aligned} \quad (\text{A8})$$

APPENDIX B: CONSISTENCY WITH LITERATURE RESULTS

In this appendix, we will recover the findings in the Refs. [50,51] for a pure external electric field at finite chemical potential and temperature in an infinite volume.

To obtain the effective Lagrangian of the model under finite temperature and density taking into account the electric field in bulk form, we start from

$$\frac{\partial \mathcal{L}_{\text{eff}}}{\partial M} = \text{Tr}[S_F(p, A^{\text{ext}})] \Rightarrow \mathcal{L}_{\text{eff}} = \int \phi(\beta, \mu, L_z \rightarrow \infty, D, \omega_E) dM + \text{const}, \quad (\text{B1})$$

where const is independent of M and will be chosen appropriately at the end of the computation.

Using the Eq. (17) in $D = 4$, we have

$$\begin{aligned} \mathcal{L}_{\text{eff}} &= \frac{4N_c}{8\pi\sqrt{4\pi}\beta} \frac{1}{\beta} \sum_{f=u}^d \int_0^\infty \frac{dS}{S^2} \sqrt{\omega_{fE} \cot(\omega_{fE}S)} \exp(-SM^2) \exp \left[\mu^2 \frac{\tan(\omega_{fE}S)}{\omega_{fE}} \right] \\ &\quad \times \theta_2 \left[\frac{2\pi\mu \tan(\omega_{fE}S)}{\beta\omega_{fE}}; \exp \left(-\frac{4\pi^2 \tan(\omega_{fE}S)}{\beta^2\omega_{fE}} \right) \right]. \end{aligned} \quad (\text{B2})$$

We can write Jacobi's theta function $\theta_2[(a \cdot t \cdot c); \exp(-a^2 \cdot c)]$ as

$$\theta_2[(atc); \exp(-a^2c)] = \frac{\sqrt{\pi}}{|a|} c^{-1/2} \exp(-t^2c) \left\{ 1 + 2 \sum_{n=1}^{+\infty} (-1)^n \exp \left[-\left(\frac{\pi^2 n^2}{a^2 c} \right) \right] \cosh \left(\frac{2\pi t n}{a} \right) \right\}.$$

For $a = 2\pi/\beta$, $t = \mu$, and $c = \tan(\omega_{fE}S)/\omega_{fE}$, the effective Lagrangian write on Eq. (B2) becomes

$$\mathcal{L}_{\text{eff}} = \mathcal{N} \sum_{f=u}^d \int_0^\infty \frac{dS}{S^2} \omega_{fE} \cot(\omega_{fE}S) \exp(-SM^2) \left\{ 1 + 2 \sum_{n=1}^{+\infty} (-1)^n \exp \left[-\left(\frac{\beta^2 n^2 \omega_{fE} \cot(\omega_{fE}S)}{4} \right) \right] \cosh(n\mu\beta) \right\}, \quad (\text{B3})$$

where \mathcal{N} is a constant positive numerical factor irrelevant to the discussions below.

Now, we can use Poisson's summation formula to show

$$\begin{aligned} &\left\{ 1 + 2 \sum_{n=1}^{+\infty} (-1)^n \exp \left[-\left(\frac{\beta^2 n^2 \omega_{fE} \cot(\omega_{fE}S)}{4} \right) \right] \cosh(n\mu\beta) \right\} \\ &= \frac{\sqrt{4\pi}}{\beta \sqrt{\omega_{fE} \cot(\omega_{fE}S)}} \sum_{n=-\infty}^{+\infty} \exp \left[-\frac{\tan(\omega_{fE}S)}{\omega_{fE}} (\omega_n - i\mu)^2 \right], \text{ being } \omega_n = \frac{\pi}{\beta} \left(2n + \frac{1}{2} \right). \end{aligned} \quad (\text{B4})$$

Thus, Eq. (B3) is recasted by

$$\mathcal{L}_{\text{eff}} = \mathcal{N} \sum_{f=u}^d \int_0^\infty \frac{dS}{S^2} \sqrt{\omega_{fE} \cot(\omega_{fE} S)} \exp(-SM^2) \frac{1}{\beta} \sum_{n=-\infty}^{+\infty} \exp \left[-\frac{\tan(\omega_{fE} S)}{\omega_{fE}} (\omega_n - i\mu)^2 \right]. \quad (\text{B5})$$

Going to Minkowski space ($S \rightarrow iS$), we have

$$\mathcal{L}_{\text{eff}} = -\mathcal{N} \sqrt{i} \sum_{f=u}^d \int_0^\infty \frac{dS}{S^2} \sqrt{\omega_{fE} \coth(\omega_{fE} S)} \exp(-iSM^2) \frac{1}{\beta} \sum_{n=-\infty}^{+\infty} \exp \left[i \frac{\tanh(\omega_{fE} S)}{\omega_{fE}} (i\omega_n + \mu)^2 \right]. \quad (\text{B6})$$

Using the expression (3.71), page 50 from Ref. [60], namely

$$\begin{aligned} \frac{1}{\beta} \sum_{n=-\infty}^{+\infty} f(p_0 = i\omega_n + \mu) &= -\frac{1}{2\pi i} \int_{-i\infty+\mu+\epsilon}^{+i\infty+\mu+\epsilon} dp_0 f(p_0) \frac{1}{1 + \exp[\beta(p_0 - \mu)]} \\ &\quad - \frac{1}{2\pi i} \int_{-i\infty+\mu-\epsilon}^{+i\infty+\mu-\epsilon} dp_0 f(p_0) \frac{1}{1 + \exp[\beta(-p_0 + \mu)]} \\ &\quad + \frac{1}{2\pi i} \oint_C dp_0 f(p_0) + \frac{1}{2\pi i} \int_{-i\infty}^{+\infty} dp_0 f(p_0), \end{aligned}$$

we see that in the present case

$$f(p_0 = i\omega_n + \mu) \equiv \exp \left[i \frac{\tanh(\omega_{fE} S)}{\omega_{fE}} (p_0)^2 \right],$$

which is analytic in the whole complex plane. Therefore, Eq. (B6) is reformulated to

$$\begin{aligned} \mathcal{L}_{\text{eff}} &= -\mathcal{N} i \sum_{f=u}^d \int_0^\infty \frac{dS}{S^2} \sqrt{\omega_{fE} \coth(\omega_{fE} S)} \exp(-iSM^2) \exp(i\pi/4) \frac{1}{2\pi} \int_{-i\infty+\mu}^{+i\infty+\mu} dp_0 f_F(p_0; \mu) \exp \left[i \frac{\tanh(\omega_{fE} S)}{\omega_{fE}} (p_0)^2 \right] \\ &\quad + \mathcal{N} i \sum_{f=u}^d \int_0^\infty \frac{dS}{S^2} \sqrt{\omega_{fE} \coth(\omega_{fE} S)} \exp(-iSM^2) \exp(i\pi/4) \frac{1}{2\pi} \int_{-i\infty}^{+\infty} dp_0 \exp \left[i \frac{\tanh(\omega_{fE} S)}{\omega_{fE}} (p_0)^2 \right], \quad (\text{B7}) \end{aligned}$$

where we used $\sqrt{i} = \exp(i\pi/4)$ and

$$f_F(p_0; \mu) \equiv \frac{1}{1 + \exp[\beta(p_0 - \mu)]} + \frac{1}{1 + \exp[\beta(-p_0 + \mu)]}.$$

After performing a Gaussian integral on the zero temperature term and defining

$$h(S) \equiv \omega_{fE} \coth(\omega_{fE} S),$$

we obtain from Eq. (B7)

$$\begin{aligned} \mathcal{L}_{\text{eff}} &= -\mathcal{N} i \sum_{f=u}^d \int_0^\infty \frac{dS}{S^2} \sqrt{h(S)} \exp(-iSM^2) \exp(i\pi/4) \frac{1}{2\pi} \int_{-i\infty+\mu}^{+i\infty+\mu} dp_0 f_F(p_0; \mu) \exp[ip_0^2/h(S)] \\ &\quad - \mathcal{N} \sum_{f=u}^d \int_0^\infty \frac{dS}{S^3} (\omega_{fE} S) \coth(\omega_{fE} S) \exp(-iSM^2) + \text{const.} \quad (\text{B8}) \end{aligned}$$

In short, we have

$$\mathcal{L}_{\text{eff}} = \mathcal{L}_{\text{vac}}(\mathbf{E}, \mathbf{0}) + \mathcal{L}^{\beta, \mu}(\mathbf{E}, \mathbf{0}) - \frac{\mathbf{E}^2}{2}, \quad (\text{B9})$$

where we renormalized “à la Schwinger” the vacuum term, that is

$$\begin{aligned} \mathcal{L}_{\text{vac}}(\mathbf{E}, \mathbf{0}) \equiv & -\mathcal{N} \sum_{f=u}^d \int_0^\infty \frac{dS}{S^3} \exp(-iSM^2) \\ & \times \left[(\omega_{fE}S) \coth(\omega_{fE}S) - 1 - \frac{(\omega_{fE}S)^2}{3} \right]. \end{aligned} \quad (\text{B10})$$

Also, we choose $\text{const} = -\mathbf{E}^2/2$.

The Eq. (B10) corresponds to Eq. (2.6) of Ref. [51] for a pure external electric field (written in Minkowski space).

The temperature-dependent term is given by

$$\begin{aligned} \mathcal{L}^{\beta, \mu}(\mathbf{E}, \mathbf{0}) = & -\mathcal{N} \sum_{f=u}^d \int_{-i\infty+\mu}^{+i\infty+\mu} \frac{dp_0}{2\pi} f_F(p_0; \mu) \\ & \times \text{Im} \left\{ i \int_0^\infty \frac{dS}{S^2} \sqrt{h(S)} \exp(-iSM^2) \right. \\ & \left. \times \exp(i\pi/4) \exp[ip_0^2/h(S)] \right\}. \end{aligned} \quad (\text{B11})$$

Equation (B11) corresponds to Eq. (2.1) of Ref. [51] for a pure external electric field (without the convergence term $-i\epsilon$). To see this, let us calculate the limit in cited Eq. (2.1):

$$\lim_{a \rightarrow 0(\mathbf{B} \rightarrow \mathbf{0})} \frac{1}{\sqrt{h(s)}} \frac{e^2}{s} \cdot a \cdot b \cdot \cot(esa) \cdot \coth(esb) = \frac{\sqrt{h(s)}}{s^2},$$

where the term $\sqrt{h(s)}/s^2$ is exactly the one in the integrand of Eq. (B11).

Thus, our chiral condensate, when replaced with Eq. (B1), leads to Eq. (B9), which is essentially the effective Lagrangian computed in Refs. [50,51].

-
- [1] W. T. Deng and X. G. Huang, *Phys. Rev. C* **85**, 044907 (2012).
- [2] G. Gräf, M. Bleicher, and Q. Li, *Phys. Rev. C* **85**, 044901 (2012).
- [3] P. B. Munzinger, V. Koch, T. Schäfer, and J. Stachel, *Phys. Rep.* **621**, 76 (2016).
- [4] U. Vogl and W. Weise, *Prog. Part. Nucl. Phys.* **27**, 195 (1991).
- [5] S. P. Klevansky, *Rev. Mod. Phys.* **64**, 649 (1992).
- [6] T. Hatsuda and T. Kunihiro, *Phys. Rep.* **247**, 221 (1994).
- [7] M. Buballa, *Phys. Rep.* **407**, 205 (2005).
- [8] D. J. Gross and A. Neveu, *Phys. Rev. D* **10**, 3235 (1974).
- [9] Y. Nambu and G. Jona-Lasinio, *Phys. Rev.* **122**, 345 (1961).
- [10] Y. Nambu and G. Jona-Lasinio, *Phys. Rev.* **124**, 246 (1961).
- [11] T. Inagaki, T. Kouno, and T. Muta, *Int. J. Mod. Phys. A* **10**, 2241 (1995).
- [12] T. Inagaki, D. Kimura, and T. Murata, *Prog. Theor. Phys.* **111**, 371 (2004).
- [13] V. A. Miransky and I. A. Shovkovy, *Phys. Rep.* **576**, 1 (2015).
- [14] J. O. Andersen, W. R. Naylor, and A. Tranberg, *Rev. Mod. Phys.* **88**, 025001 (2016).
- [15] Q. Wang, Y. Xiq, and H. Zong, *Mod. Phys. Lett. A* **33**, 1850232 (2018).
- [16] L. M. Abreu, E. B. S. Corrêa, and E. S. Nery, *Physica (Amsterdam)* **572A**, 125885 (2021).
- [17] L. M. Abreu, E. B. S. Corrêa, and E. S. Nery, *Phys. Rev. D* **105**, 056010 (2022).
- [18] R. Zhang, Wj. Fu, and Yx. Liu, *Eur. Phys. J. C* **76**, 307 (2016).
- [19] S. S. Avancini, R. L. S. Farias, and W. R. Tavares, *Phys. Rev. D* **99**, 056009 (2019).
- [20] F. C. Khanna, A. P. C. Malbouisson, J. M. C. Malbouisson, and A. E. Santana, *Thermal Quantum Field Theory: Algebraic Aspects and Applications* (World Scientific, Singapore, 2009).
- [21] F. C. Khanna, A. P. C. Malbouisson, J. M. C. Malbouisson, and A. E. Santana, *Phys. Rep.* **539**, 135 (2014).
- [22] E. B. S. Corrêa, C. A. Linhares, A. P. C. Malbouisson, J. M. C. Malbouisson, and A. E. Santana, *Eur. Phys. J. C* **77**, 261 (2017).
- [23] E. B. S. Corrêa, C. A. Linhares, and A. P. C. Malbouisson, *Int. J. Mod. Phys. B* **32**, 1850091 (2018).
- [24] I. A. Shovkovy, *Lect. Notes Phys.* **871**, 13 (2013).
- [25] L. M. Abreu, E. B. S. Corrêa, C. A. Linhares, and A. P. C. Malbouisson, *Phys. Rev. D* **99**, 076001 (2019).
- [26] V. P. Gusynin, V. A. Miransky, and I. A. Shovkovy, *Nucl. Phys.* **B462**, 249 (1996).
- [27] D. P. Menezes, M. Benghi Pinto, S. S. Avancini, A. Pérez Martínez, and C. Providência, *Phys. Rev. C* **79**, 035807 (2009).
- [28] B. Chatterjee, H. Mishra, and A. Mishra, *Phys. Rev. D* **84**, 014016 (2011).
- [29] M. D’Elia, S. Mukherjee, and F. Sanfilippo, *Phys. Rev. D* **82**, 051501(R) (2010).
- [30] A. Ahmad and A. Raya, *J. Phys. G* **43**, 065002 (2016).

- [31] A. Martínez and A. Raya, *Nucl. Phys.* **B934**, 317 (2018).
- [32] M. Ferreira, P. Costa, O. Lourenço, T. Frederico, and C. Providência, *Phys. Rev. D* **89**, 116011 (2014).
- [33] A. Bandyopadhyay and R. L. S. Farias, *Eur. Phys. J. Special Topics* **230**, 719 (2021).
- [34] G. S. Bali, F. Bruckmann, G. Endrödi, F. Gruber, and A. Schäfer, *J. High Energy Phys.* **04** (2013) 130.
- [35] F. Bruckmann, G. Endrödi, and T. G. Kovács, *J. High Energy Phys.* **04** (2013) 112.
- [36] N. Chaudhuri, S. Ghosh, S. Sarkar, and P. Roy, *Phys. Rev. D* **99**, 116025 (2019).
- [37] *Strong Interacting Matter in Magnetic Fields*, edited by D. Kharzeev, K. Landsteiner, A. Schmitt, and H. U. Yee, Lecture Notes in Physics Vol. 871 (Springer-Verlag, Berlin-Heidelberg, 2013).
- [38] E. J. Ferrer, V. de la Incera, and X. J. Wen, *Phys. Rev. D* **91**, 054006 (2015).
- [39] S. Mao, *Phys. Lett. B* **758**, 195 (2016).
- [40] J. O. Andersen, *Eur. Phys. J. A* **57**, 189 (2021).
- [41] N. Mueller and J. M. Pawłowski, *Phys. Rev. D* **91**, 116010 (2015).
- [42] V. P. Pagura, D. G. Dumm, S. Noguera, and N. N. Scoccola, *Phys. Rev. D* **95**, 034013 (2017).
- [43] R. L. S. Farias, K. P. Gomes, G. Krein, and M. B. Pinto, *Phys. Rev. C* **90**, 025203 (2014).
- [44] L. M. Abreu, E. B. S. Corrêa, and E. S. Nery, [arXiv:2211.11083v1](https://arxiv.org/abs/2211.11083v1).
- [45] T. Inagaki, Y. Matsuo, and H. Shimoji, *Prog. Theor. Exp. Phys.* **013B09**, 1 (2022).
- [46] T. Misumi and T. Kanazawa, *J. High Energy Phys.* **06** (2014) 181.
- [47] E. Cavalcanti, C. A. Linhares, and A. P. C. Malbouisson, *Int. J. Mod. Phys. A* **33**, 1850008 (2018).
- [48] E. B. S. Corrêa, C. A. Linhares, and A. P. C. Malbouisson, *Phys. Lett. A* **377**, 1984 (2013).
- [49] J. Schwinger, *Phys. Rev.* **82**, 664 (1951).
- [50] P. Elmfors and B.-S. Skagerstam, *Phys. Lett. B* **348**, 141 (1995); **376**, 330(E) (1996).
- [51] P. Elmfors and B.-S. Skagerstam, *Phys. Lett. B* **427**, 197 (1998).
- [52] G. Cao and X. G. Huang, *Phys. Rev. D* **93**, 016007 (2016).
- [53] E. T. Whittaker and G. N. Watson, *A Course of Modern Analysis*, 4th ed. (Cambridge University Press, New York, 1927).
- [54] *Handbook of Mathematical Functions with Formulas, Graphs, and Mathematical Tables*, edited by M. Abramowitz and I. A. Stegun (National Bureau of Standards, Washington D.C., 1970), ninth Printing.
- [55] L. Wang, G. Cao, X. G. Huang, and P. Zhuang, *Phys. Lett. B* **780**, 273 (2018).
- [56] A. Ahmad, *Chin. Phys. C* **45**, 073109 (2021).
- [57] G. S. Bali, F. Bruckmann, G. Endrödi, Z. Fodor, S. D. Katz, and A. Schafer, *Phys. Rev. D* **86**, 071502 (2012).
- [58] E. B. S. Corrêa, C. A. Bahia, and J. A. Lourenço, *Can. J. Phys.* **100**, 1 (2022).
- [59] E. B. S. Corrêa and J. E. Oliveira, *Rev. Bras. Ens. Fís.* **37**, 3302 (2015).
- [60] J. I. Kapusta and C. Gale, *Finite-Temperature Field Theory Principles and Applications*, 2nd ed. (Cambridge University Press, New York, 2006).